Asian Journal of Chemistry; Vol. 35, No. 11 (2023), 2739-2748

ASIAN JOURNAL OF CHEMISTRY

https://doi.org/10.14233/ajchem.2023.30234

Optimization of Ca^{2+} Removal from Cooling Tower Water using Amberlite IR120 and Amberjet 1200 Resins: A Response Surface Methodology Study

ROBERT MBEDZI[1,*], HILARY RUTTO[1], TUMISANG SEODIGENG[1] and LINDA SIBALI[2]

[1]Clean Technology and Applied Materials Research Group, Department of Chemical and Metallurgical Engineering, Vaal University of Technology, Private Bag X021, South Africa

[2]Department of Environmental Sciences, College of Agriculture and Environmental Sciences, UNISA, Florida, 1709, South Africa

*Corresponding author: E-mail: robertm@vut.ac.za

Received: 1 August 2023; *Accepted*: 24 September 2023; *Published online*: 31 October 2023; AJC-21430

In present study, the removal of Ca^{2+} from cooling tower water using Amberlite IR120 and Amberjet 1200 was optimized using the response surface methodology (RSM). The effect of operational parameters such as contact time (min), pH, dosage (mL), concentration (mg/L) and temperature (K) were investigated using a central composite design. The regeneration of the Amberlite IR120 and Amberjet were also studied. The study aimed to apply RSM to investigate and optimize the ion exchange operating parameters. Furthermore, the second-order empirical model was developed and correlated sufficiently to the ion exchange experimental data. The optimal ion exchange operating conditions for Amberlite IR120 and Amberjet 1200 were found to be: contact time was 120 min, dosage of 150 mL, the initial pH level of 2, a concentration of 4,00 mg/L and temperature of 343 K. Regeneration of Amberlite IR120 and Amberjet 1200 using 0.5 M NaCl stripping solution initially showed an increase in % Ca^{2+} and Mg^{2+} removal, then a decrease in subsequent cycles.

Keywords: Amberlite IR120, Amberjet 1200, Cooling tower water, Response surface methodology, Ca^{2+}, Mg^{2+}, Regeneration.

INTRODUCTION

The global increase in industrialization and quick development resulting from the industrial revolution has led to a continuous rise in the output of wastewater. This has necessitated the implementation of stringent laws and has created a highly competitive environment. However, industries have already taken more environmentally sustainable and economically feasible actions, such as wastewater reuse and recycling. Most of the industrial-sector effluent discharges, such as metal grinding, welding, steel production, plating and mining, are critical polluting sources of heavy metals in soil and water [1,2]. This has contributed remarkably to the increase in the concentration of harmful heavy-metal ions in waters that could be a source of some dangerous disadvantages for aquatic flora, animals and even humans [3,4].

Environmental agencies and authorities have set strict regulations to limit heavy metals in wastewater below the maximum acceptable concentration levels because of their health and toxicological effects. These strict regulations have accelerated research into new environmental friendly technologies that can reduce concentrations of heavy metals in the wastewater discharged to be below the maximum to low limit [5].

The standard methods to remove heavy metals from aqueous solutions are reverse osmosis, ultrafiltration, chemical precipitation, adsorption and ion exchange [6-12]. Among these heavy metal removal processes, the ion exchange process (IEX) seems to be very effective in reducing the concentration of heavy metals because it is environmentally friendly, economically viable, selective, less sludge volume produced and meets restricted discharge specifications and the ion exchange resin can be quickly recovered and reused by regeneration operation [13]. The ion exchange process process involves transferring a solid matrix, which releases ions of the same charge [14].

Toxic metals damage the plasma cell membrane system in reverse osmosis. The interaction of heavy metals and membrane functional groups disrupt the membrane's integrity. The sulphhydryl groups of proteins and the hydroxyl part of phospholipids are easily bounded by metal ions [15]. They can also replace the calcium ions at essential sites on the cell membranes

[16]. The ionic equilibrium and hence the functions of numerous enzymes essential for primary cell metabolism are disrupted as a result of this procedure, which increases non-specific membrane permeability while simultaneously decreasing particular transporting activities.

The regeneration ion exchange resin is conducted to reuse the exhausted resin to its normal ionic phase. It is usually regenerated with highly concentrated electrolyte solutions (NaCl or HCl). Several researchers have reviewed this regeneration technology's applications in different areas [17]. When all the available Na^+ ions have been replaced by calcium or magnesium ions, the resin must be re-charged by eluting the Ca^{2+} ions using a solution of sodium chloride or sodium hydroxide, depending on the type of resin used. The waste waters eluted from the ion exchange column containing the unwanted calcium and magnesium salts are typically discharged to the sewerage system.

The ion exchange resins have several commercial and industrial uses, particularly in water purification and removal of ions at very low concentrations in chemical processes [18]. Polymeric resins having strongly acid sulfonic or weakly acid carboxylic functionalities are usually used in ion exchange processes [19,20]. The exchange of Ca^{2+} and Mg^{2+} from $LiHCO_3$ was studied with Amberjet 1200 Na^+. Applications of polymeric resins containing iminodiacetate have been investigated from aqueous solutions to recover Ca^{2+} and Mg^{2+} [21-23]. Studies have used exchange resin such as Ca^{2+} removal and magnesium adsorption [24]. The results show that polymeric resin has proved effective in removing heavy metals. Ion exchange resins are generally insoluble polymeric materials manufactured using suspension polymerization using styrene and divinylbenzene (DVB) that carry ion exchangeable functional groups. These ions can be exchanged with stoichiometrically equivalent amounts of the same sign.

Response surface methodology (RSM) is a collection of mathematical and statistical techniques useful for the modeling and analysis of problems in which several variables influence a response of interest and the objective is to optimize this response [25]. The current study examined the feasibility of using ion exchange resin to remove Ca^{2+} and Mg^{2+} and its regeneration efficiency. The effect of pH, temperature, contact time and amount of resins was investigated using response surface methodology (RSM).

EXPERIMENTAL

All the solutions were prepared using analytical grade chemicals and deionized water was used throughout the experiments.

Experimental analysis: The experiments carried out in this study were conducted using Amberjet 1200 and Amberlite IR 120 resins. These experiments were carried out by varying the set points conditions of process variables, noting the outcomes and analyzing their effects on removal percen-tages of heavy metals.

Characterization: Ion exchange resins *viz.* Amberjet 1200 and Amberlite IR 120 were obtained from Dow Chemicals, South Africa. Both resins were washed three times with solutions of, respectively, 1.0 mol/HCl and 1.0 mol/NaOH before it was used to remove possible organic and inorganic impurities. It was then washed with distilled water and converted to H^+ from Na^+ by flushing in the fixed bed with 1.0 mol/L HCl. The resin H^+ form will be washed with water and be used throughout the experiment.

Preparation of stock solutions: The solution of Ca^{2+} with a concentration range of 400-800 mg/L and Mg^{2+} with a concentration range of 100-400 mg/L were prepared by dissolving an analytical grade of $CaCl_2{\cdot}2H_2O$ and $MgCl_2{\cdot}6H_2O$, respectively. Stock solutions of 1000 mg/L of Ca^{2+} and Mg^{2+} were prepared by dissolving 2.998 g of $CaCl_2{\cdot}2H_2O$ and 3.654 g of $MgCl_2{\cdot}6H_2O$ in 1 L of deionized water.

Experimental setup: Column experiments were performed using a glass tube of 3 cm diameter and 28 cm height. The schematic diagram of the experimental setup is shown in Fig. 1. The ion exchange process was carried out in column systems, which consists of a vertical column packed with exchange resins through which the feed solution was continuously pumped into the column.

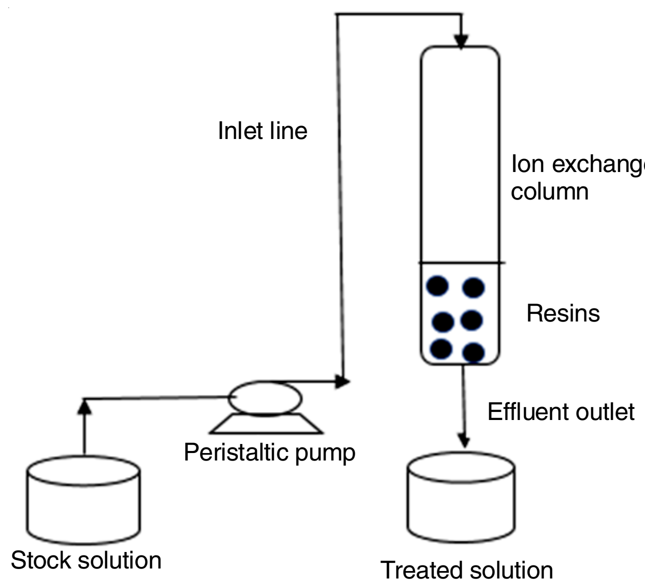

Fig. 1. Experimental setup for ion exchange column

Experimental procedure: A graduated 200 mL beaker measuring cylinder was used to measure the amount of Amberjet 1200 and Amberlite IR 120 resins. The resins were transferred to a resin testing glass column of 3 cm diameter; the column was used as an ion exchange (IEX) column throughout the laboratory scale experimental procedure. The stock solutions were continuously pumped from the glass beaker into the top of IEX column.

A hot plate stirrer controlled the reaction temperature. The pH of the reaction mixture was determined using a pH electrode inserted in the solution and connected to a pH 200 1/8DIN pH controller. The controller has a specific pH range of pH 0.01. When the pH exceeded the set value, the pump was activated to add acid to the reaction vessel and lower the pH value to the set point. A sample was removed, filtered and analyzed for calcium and magnesium ions using the atomic absorption spectrophotometer (AAS).

Regeneration of the ion exchange resin is used to recover the ion exchange capabilities of exhausted resins. In this study, preliminary experiments were conducted to evaluate the regeneration capacity of the resins by using 0.5 M NaCl in the exchange column. After each run, the column was regenerated by 0.5 M NaCl as a stripping solution. After the stripping stage, the column was then washed with deionized water. The percentage removal of Ca^{2+} and Mg^{2+} from aqueous solution by Amberjet 1200 and Amberlite IR 120 resins was calculated according to eqn. 1:

$$\text{Removal (\%)} = \frac{C_i - C_f}{C_f} \times 100 \quad (1)$$

where C_i and C_f are the initial and final concentrations (mg/L), respectively.

Design experiments: Response surface methodology (RSM) evaluates the interactions between the system variables and the variable response [26]. Based on past studies, the process variables that mainly affect the system's efficiency and performance, such as contact time (min), concentration (mg/L), resins dosage (mL), temperature (K) and pH, were investigated. Therefore, the influence of these reaction conditions on the removal of Ca^{2+} from cooling tower water was investigated using RSM. The experimental design used in the current study was the full factorial with axial points. It was selected due to its ability to examine the results, changing several variables simultaneously, thereby revealing the interdependency of the variables. While this design is complex, the advantages are it is less costly and less time-consuming.

Table-1 shows the factorial design setup consisting of five variables (k = 5) and the coded variables, determined by using eqn. 1, were set at five levels: -1 (minimum), 0 (central) and +1 (maximum). After conducting the experiments according to the experimental matrix (Table-1), response surface modeling was conducted by applying the central composite design (CCD), using Design Expert® Software of Stat-Ease Inc. (version 6.0.6), to model and optimize the reaction conditions.

$$x_i = \left(\frac{z_i - z_i^o}{\Delta z_i}\right) \quad (2)$$

where x_i is the coded level, Δz_i is the distance between the actual value at the central point and the real value in the low or high level of a variable (step change), z_i is the real value and z_i^o is the real value in the central point.

TABLE-1
SURFACE RESPONSE METHODOLOGY EXPERIMENTAL RANGE AND LEVELS OF VARIABLES CHOSEN FOR THIS STUDY

Variable	Coding	Levels		
		-1	0	1
Contact time (min)	A	30	75	120
pH	B	2	4	7
Concentration (mg/L)	C	400	600	800
Dosage (mL)	D	50	100	150
Temperature (K)	E	273	308	343

In CCD, the major operating parameters contact time (A), pH level (B), concentration (C), dosage (D) and temperature (E) were considered as independent variables, whereas Ca^{2+} removed in % were used as variables of response for Amberlite IR1200 and Amberjet 120. A sequential model fitting test was conducted to select a suitable model. A second-order polynomial model (eqn. 3) was used to fit the data found from the 32 experiments. Analysis of variance (ANOVA) was used to attain the interaction between the process variables and the response parameter, determine the statistical significance and reliability of each term in the polynomial model and determine the graphical analysis of the data. The regression coefficients in the polynomial equation were used to produce 3D surface response and contour plots. The process variables were optimized by solving the regression equation and graphical analysis of the data.

$$y = \beta_o + \sum_{i=1}^{k} \beta_i x_i + \sum_{i=1}^{k} \beta_{ii} x_i^2 + \sum_{1 \le i \le j}^{k} \beta_{ij} x_i x_j + e \quad (3)$$

where β_o is the constant term, k is the number of variables, x_i symbolizes the variables, e is the residual error observed in the response and β_i signifies the coefficients of the linear variables; β_y signifies the coefficients of the interaction parameters and $x_i x_i$ represents the interaction between the different variables.

RESULTS AND DISCUSSION

Table-2 shows the experimental response for both Amberlite IR 1200 and Amberjet 120 and the combination of the respective system variables. The highest % Ca^{2+} removed for Amberlite IR1200 and Amberjet 120 were found to be 99.65 and 99.36%, while the lowest % Ca^{2+} were 25.63 and 21.56.

Stat-Ease Inc's Design Expert® Program was used to determine the expected using the final empirical second-order model (eqns. 4 and 5) regarding coded variables. Although there was a slight deviation in some other experimental runs, the predicted values showed a sufficient correlation to the experimental values. Several models were fitted with the experimental data (cubic, quadratic and linear). Through their subsequent ANOVA, however, it was found that the empirical second-order model best described the removal of Ca^{2+} from cooling tower water using both resins.

$$Y_{Ca}\text{ (Amberlite)} = 94.54 + 2.13\,A - 2.57B - 3.28\,C + 1.29\,D + 1.18\,E - 2.75\,B^2 - 2.01\,AD - 1.59\,BC - 1.60\,B\,D + 0.82\,DE \quad (4)$$

$$Y_{Ca}\text{ (Amberjet)} = 97.19 - 3.62\,B + 1.50D + 3.10E - 4.16D^2 + 3.92BC + 2.42BE - 1.13CE \quad (5)$$

Contact time (min), pH, concentration (mg/L), dosage (mL) and temperature (K) are expressed by A, B, C, D and E, respectively. The positive sign suggests a synergistic effect; in eqns. 4 and 5, the negative sign indicates an antagonistic effect.

The ANOVA and the significance test were used to assess the adequacy of the empirical second-order model. The significance method was used to determine the statistical second-order model's regression coefficients. The ANOVA test has been used to determine the importance of the second-order statistical model [26]. The evaluation was performed by asses-

TABLE-2
EXPERIMENTAL DESIGN AND RESPONSE VALUES

Run	A: Contact time (min)	B: pH	C: Conc. (mg/L)	D: Dosage (mL)	E: Temp. (K)	% Ca (Amberlite)	% Ca (Amberjet)
1	120.00	7.00	800.00	50.00	273.00	88.08	82.27
2	30.00	2.00	400.00	150.00	273.00	93.41	97.80
3	75.00	4.50	400.00	100.00	308.00	98.44	96.98
4	120.00	2.00	800.00	150.00	273.00	91.83	91.25
5	75.00	4.50	600.00	100.00	308.00	94.33	95.75
6	75.00	4.50	600.00	100.00	273.00	92.45	96.22
7	75.00	4.50	600.00	100.00	308.00	94.24	98.31
8	75.00	4.50	800.00	100.00	308.00	88.19	93.69
9	30.00	4.50	600.00	100.00	308.00	92.25	97.11
10	120.00	7.00	400.00	150.00	273.00	90.19	75.80
11	120.00	2.00	400.00	150.00	343.00	99.10	99.01
12	75.00	7.00	600.00	100.00	308.00	89.01	92.20
13	30.00	2.00	800.00	50.00	273.00	83.65	85.25
14	75.00	4.50	600.00	100.00	308.00	95.81	98.40
15	120.00	7.00	400.00	50.00	343.00	95.42	88.28
16	120.00	4.50	600.00	100.00	308.00	94.74	91.68
17	75.00	4.50	600.00	50.00	308.00	92.28	92.19
18	120.00	7.00	800.00	150.00	343.00	81.84	92.97
19	30.00	7.00	400.00	50.00	273.00	85.91	72.67
20	75.00	2.00	600.00	100.00	308.00	94.79	99.06
21	120.00	2.00	800.00	50.00	343.00	91.87	87.50
22	75.00	4.50	600.00	100.00	308.00	94.02	98.89
23	75.00	4.50	600.00	100.00	308.00	93.85	99.11
24	75.00	4.50	600.00	100.00	343.00	97.60	98.31
25	75.00	4.50	600.00	100.00	308.00	93.99	96.44
26	30.00	7.00	800.00	150.00	273.00	79.30	87.50
27	75.00	4.50	600.00	150.00	308.00	96.41	93.13
28	120.00	2.00	400.00	50.00	273.00	94.11	91.80
29	30.00	7.00	400.00	150.00	343.00	94.19	89.23
30	30.00	2.00	400.00	50.00	343.00	86.56	97.01
31	30.00	7.00	800.00	50.00	343.00	79.34	93.53
32	30.00	2.00	800.00	150.00	343.00	94.22	90.11

sing the probability value (P) and the Fisher test (F) for each model coefficient of regression. The meaning of the process variables interaction is defined by the Fisher test, thus forming a correlation between the process variables interaction [27]. F value of 24.04 and P value < 0.0001 for Amberlite (Y_{ca}) (Table-1) and F value of 17.31 and P value < 0.0001 for Amberjet (Y_{ca}) (Table-2) suggests that the model was suitable in the analysis of the experimental data. Prob > F values below 0.0001 show that the terms of the model are significant. Therefore, model terms with P-values below 0.05 are considered statistically significant.

In Tables 3 and 4, an analysis of variance (ANOVA) was performed to illustrate the effect of each variable, and the results are presented below. The P-value was found to be 0.14 for Y ($_{\text{Amberjet}}$) due to lack of fit, suggesting that it was statistically insignificant (Table-3). However, the P value for Y ($_{\text{Amberlite}}$) was 0.0493, showing that it was statistically significant (Table-4). The determination coefficient (R^2) for Y($_{\text{Amberlite}}$) and Y($_{\text{Amberjet}}$) were found to be 0.937 and 0.913, respectively which means that both the Y($_{\text{Amberlite}}$) and Y($_{\text{Amberjet}}$) models can describe 93.7% and 91.3% of the variations found in the response variable, while the residual variability is 6.3% and 8.7%, respectively [28]. The most ineffective variables were the correlations between the contact time/concentration (AC) and pH/temperature (BE) for Y($_{\text{Amberlite}}$), with the F value of 0.099 and 0.080, respectively. In contrast, Y (Amberjet) ineffective variables resulted in an F value of 0.03 for the correlations between contact time/temperature and concentration/dosage.

Fig. 2a-b shows the good linear correlations, normal distribution and independence of experimental errors between the actual and predicted % Ca^{2+} removal calculated from eqns. 4 and 5. Random scatter indicates the proper arrangement between the predicted and experimental data, meaning that this model best fits the relationship between the system variables.

Three-dimensional (3D) surface response: Through plotting 3D response surface plots, the interaction between system variables can be better understood. These 3D surface plots are the graphical demonstrations of the second-order empirical model established. They help to analyze the interaction between the process variables and determine the optimum of each level [29].

Interaction of contact time and pH: The circular nature of contour plots in Figs. 3a and 4a demonstrate a significant interaction between contact time and pH on removing Ca^{2+} from cooling tower water. Figs. 3b and 4b show that the two variables significantly remove Ca^{2+} using both Amberlite IR 1200 and Amberjet 1200. It was observed that there was an increase in % removal of Ca^{2+} from 65.5 to 95.2 (Fig. 3a) using Amberlite IR120 and 67.36 to 96.32 (Fig. 4a) using Amberjet 1200 with

TABLE-3
ANOVA RESULTS OF REGRESSION MODEL FOR AMBERLITE (Y_{ca})

Source	Sum of squares	DF	Mean square	F value	Prob > F	
Model	802.36	20	40.12	24.04	< 0.0001	Significant
A	81.63	1	81.63	48.91	< 0.0001	
B	118.94	1	118.94	71.26	< 0.0001	
C	193.49	1	193.49	115.93	< 0.0001	
D	30.03	1	30.03	17.99	0.0014	
E	25.04	1	25.04	15.00	0.0026	
A^2	3.31	1	3.31	1.98	0.1865	
B^2	18.65	1	18.65	11.17	0.0066	
C^2	4.45	1	4.45	2.66	0.1308	
D^2	0.25	1	0.25	0.15	0.7084	
E^2	0.33	1	0.33	0.20	0.6643	
AB	0.32	1	0.32	0.19	0.6711	
AC	0.16	1	0.16	0.099	0.7595	
AD	64.68	1	64.68	38.75	< 0.0001	
AE	4.03	1	4.03	2.42	0.1485	
BC	40.65	1	40.65	24.36	0.0004	
BD	40.93	1	40.93	24.52	0.0004	
BE	0.13	1	0.13	0.080	0.7829	
CD	7.07	1	7.07	4.24	0.0640	
CE	3.28	1	3.28	1.96	0.1887	
DE	10.80	1	10.80	6.47	0.0273	
Residual	18.36	11	1.67			
Lack of fit	15.73	6	2.62	4.99	0.0493	Significant
Pure error	2.63	5	0.53			
Cor total	820.72	31				
R^2 = 0.9776						
Adjusted	R^2 = 0.937					

TABLE-4
ANOVA RESULTS OF REGRESSION MODEL FOR AMBERJET (Y_{ca})

Source	Sum of squares	DF	Mean square	F value	Prob > F	
Model	1308.41	20	65.42	17.31	< 0.0001	Significant
A	4.24	1	4.24	1.12	0.3124	
B	236.33	1	236.33	62.55	< 0.0001	
C	0.72	1	0.72	0.19	0.6720	
D	40.29	1	40.29	10.66	0.0075	
E	173.07	1	173.07	45.81	< 0.0001	
A^2	13.33	1	13.33	3.53	0.0871	
B^2	2.97	1	2.97	0.79	0.3943	
C^2	4.75	1	4.75	1.26	0.2862	
D^2	42.60	1	42.60	11.28	0.0064	
E^2	0.72	1	0.72	0.19	0.6706	
AB	0.28	1	0.28	0.073	0.7916	
AC	0.14	1	0.14	0.036	0.8520	
AD	3.47	1	3.47	0.92	0.3582	
AE	0.013	1	0.013	3.500E-003	0.9539	
BC	245.71	1	245.71	65.03	< 0.0001	
BD	3.46	1	3.46	0.92	0.3592	
BE	93.53	1	93.53	24.76	0.0004	
CD	0.034	1	0.034	9.058E-003	0.9259	
CE	20.37	1	20.37	5.39	0.0404	
DE	16.49	1	16.49	4.37	0.0607	
Residual	41.56	11	3.78			
Lack of fit	32.00	6	5.33	2.79	0.1400	Not significant
Pure error	9.56	5	1.91			
Cor total	1349.97	31				
R^2	0.9692					
Adjusted R^2	0.913					

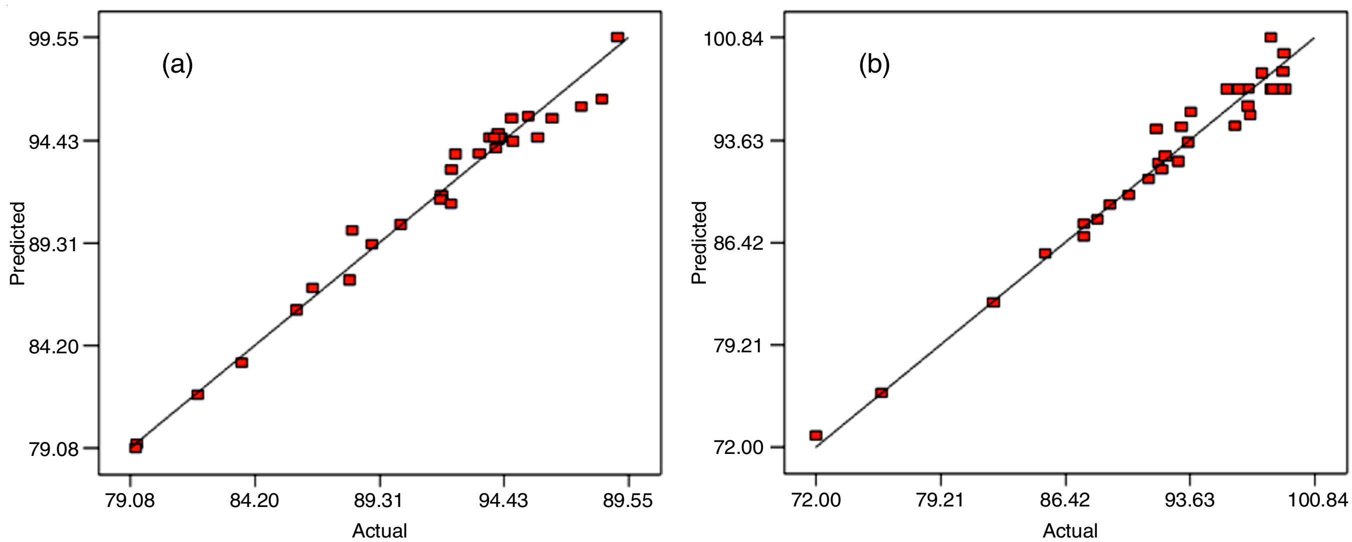

Fig. 2. Relationship between the actual and predicted values for Ca^{2+} removal (a) Amberlite IR120 and (b) Amberjet 1200

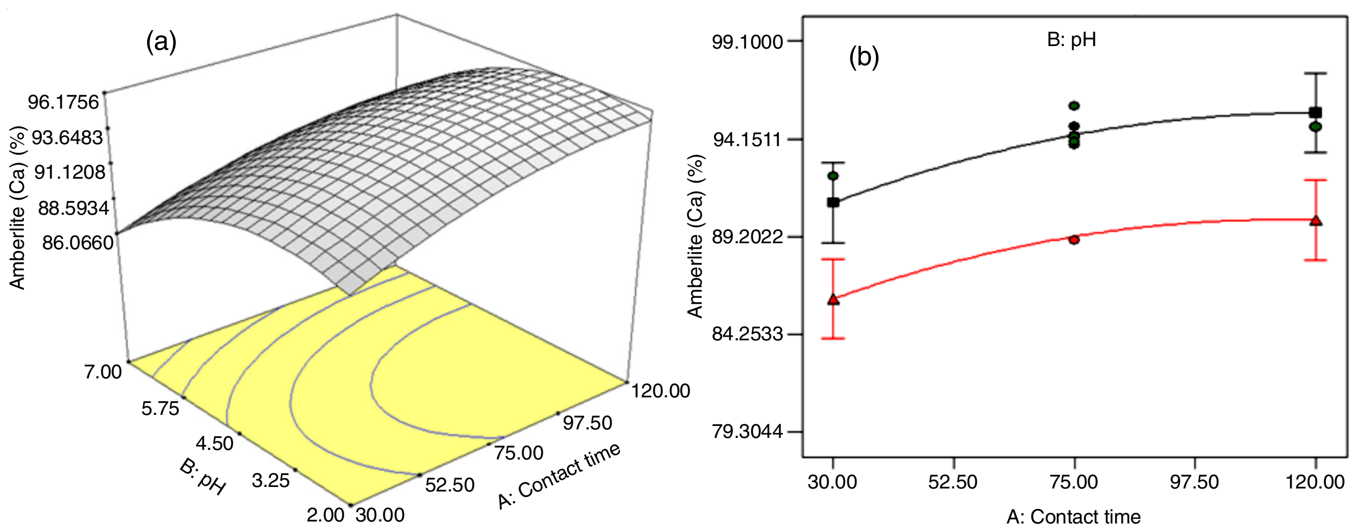

Fig. 3. Effect of pH and contact time on the removal of Ca^{2+} using Amberlite: (a) surface response method and (b) two-dimensional plot

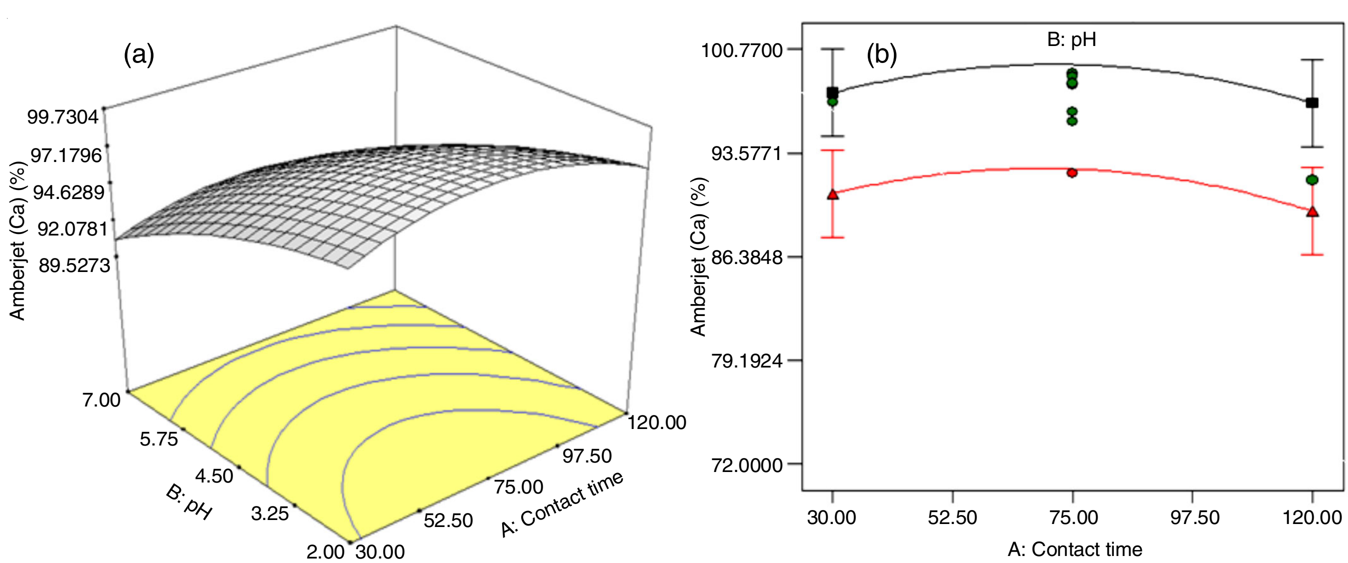

Fig. 4. Effect of pH and contact time on the removal of Ca^{2+} using Amberjet: (a) surface response method and (b) two-dimensional plot

an increase in contact time from 30 to 120 min. On the other hand, there was an increase of % removal of Ca^{2+} from 65.5 to 95.2 (Fig. 4a) using Amberlite and 67.36 to 96.32 using Amberjet 1200 with a pH decrease from 7 to 2. This means that the active surfaces on the resins were fully occupied and the process achieved equilibrium when the process reached a reaction time of 100 min for Amberlite IR1200 and 120 min for Amberjet 1200. The OH groups change resins and their derivatives negatively in an aqueous solution. Therefore, their electrostatic attraction to the catalyst particles is expected to be more favourable in acidic conditions and repulsive in alkaline conditions. Subsequently, the pH results revealed that removing Ca^{2+} in acidic conditions was preferable compared to alkaline conditions.

Interaction of temperature and pH: Figs. 5 and 6 show the effect of temperature and pH on removing Ca^{2+} from cooling tower water using Amberlite IR120 and Amberjet 1200, respectively. The effect of temperature and pH play a vital role in removing Ca^{2+} from cooling water. An increase in % Ca^{2+} removal using Amberlite IR120 from 86.4 to 94.6 with an increase of temperature from 273K to 343K, as shown in Fig. 5a. It was also observed that there was an increase in % Ca^{2+} removal using Amberjet 1200 from 80.7 to 94.2 with an increase of temperature from 273 K to 343 K. The temperature of the solution can affect the solution/solid interface and determine the resin's ability for a given initial concentration reported that high temperature increases energy, resulting in a molecular collision and decreases the probability of attaching heavy metals to the available active sites [30]. The contour indicates that the effect of temperature is more critical than response pH and Interaction occurs between them.

Interaction of temperature and dosage: The interaction between the temperature and resin dosage in the removal of

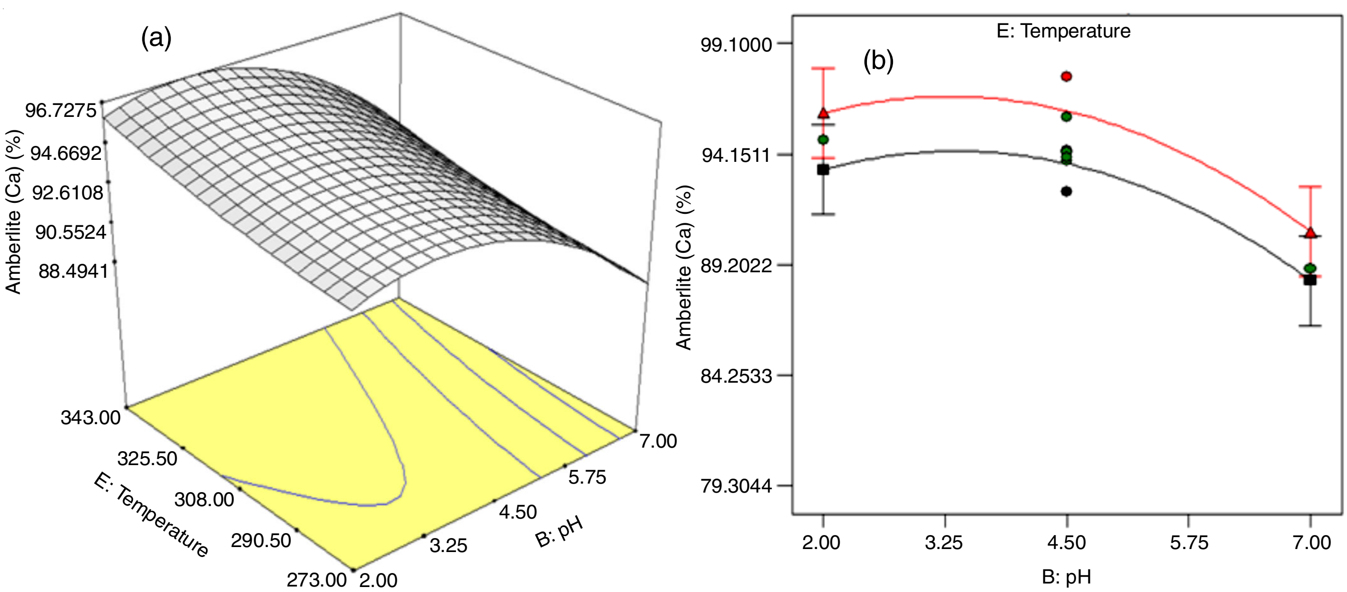

Fig. 5. Effect of temperature and pH on the removal of Ca^{2+} using Amberlite: (a) surface response method and (b) two-dimensional plot

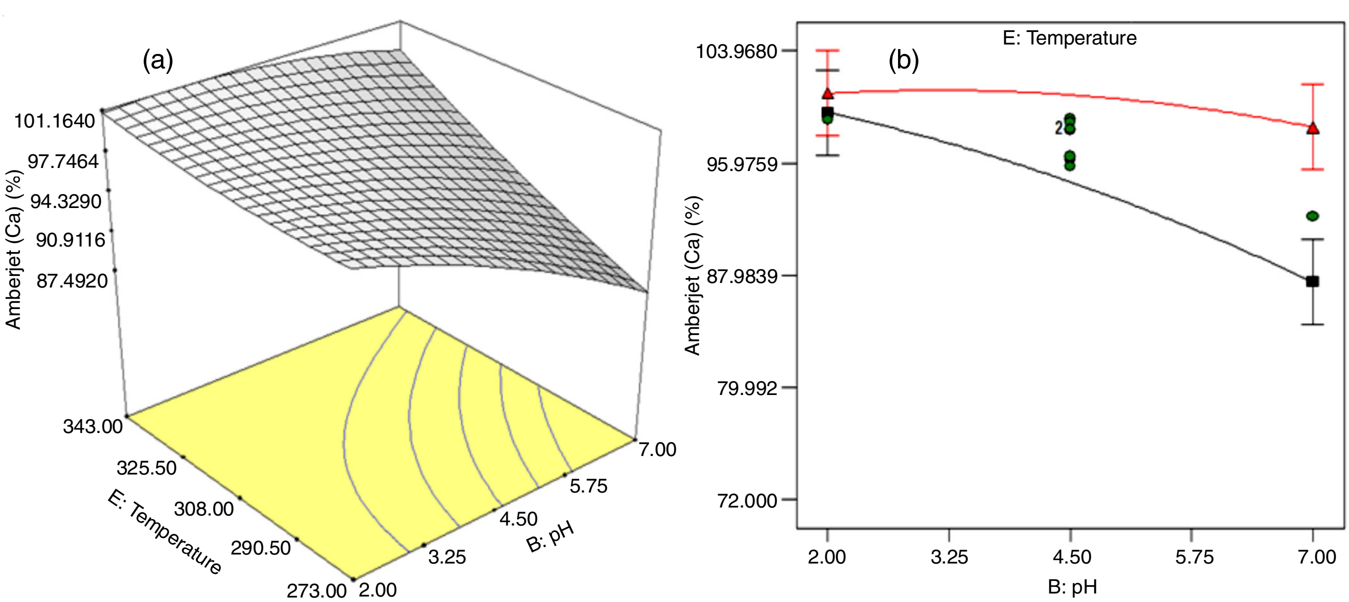

Fig. 6. Effect of temperature and pH on the removal of Ca^{2+} using Amberjet: (a) surface response method and (b) two-dimensional plot

Ca^{2+} from cooling tower water using both Amberlite IR1200 and Amberjet 120 is illustrated in Figs. 7 and 8. Resin dosage played an essential role in determining the capacity of the adsorbent for a given initial concentration of the adsorbate in the operation conditions. There was an increase in % removal of Ca^{2+} from 70.2 to 94.81 using Amberlite IR1200 (Fig. 7a) when the resins dosage increased from 50 to 150 mL. Another increase in % removal of Ca^{2+} using Amberjet 1200 from 71.23 to 94.44 with an increase of resin dosage from 50 to 150 mL was observed. An increase in Ca^{2+} percentage removal with an increase in adsorbent dosage is due to the greater availability of the exchangeable sites or surface area at higher adsorbent concentrations. The contour indicates that the effect of temperature is more critical than the response resin dosage and interaction occurs between them.

Regeneration of Amberlite IR1200 and Amberjet 1200: The regeneration of Amberlite IR1200 and Amberjet 120 resins plays a vital role in the ion exchange process as it can extract adsorbed metals from the resins, which can then be added back to the process flow reported that regeneration regulates reversibility and reusability of the resins materials [30].

Figs. 9 and 10 illustrate the regeneration of Amberlite IR1200 and Amberjet120 of Ca^{2+} and Mg^{2+} from cooling tower water using 0.5M NaCl stripping solution. All regeneration experiments were conducted at pH = 3, dosage = 15 mL, temp. = 273 K and concentration of Ca^{2+} = 600 mg/L

The first regeneration for both Amberlite IR1200 and Amberjet 1200 showed an increase in the removal of Ca^{2+} and Mg^{2+}, accompanied by a decrease in subsequent cycles. The highest % Ca removal of the initial run was 86.56, followed by an increase to 98.78 of the first regeneration for Amberlite IR1200 (Fig. 9a). It was also observed that the highest % Ca removal of the initial run was 85.56, whereas the first regeneration increased to 89.25 (Fig. 9b). The second, third and fourth regeneration using Amberlite IR1200 for % Ca removal were found to be 86.56, 80.56 and 65.23, respectively. Fig. 9b shows that the highest % Ca removal for second, third and fourth regeneration using Amberjet 120 was 87.78, 80.67 and 56.45, respectively.

The highest % Mg^{2+} removal for the initial run using Amberlite IR1200 and Amberjet 120 were 85.56 and 86.8, as shown in Fig. 10a-b. The highest % Mg^{2+} removal of the initial,

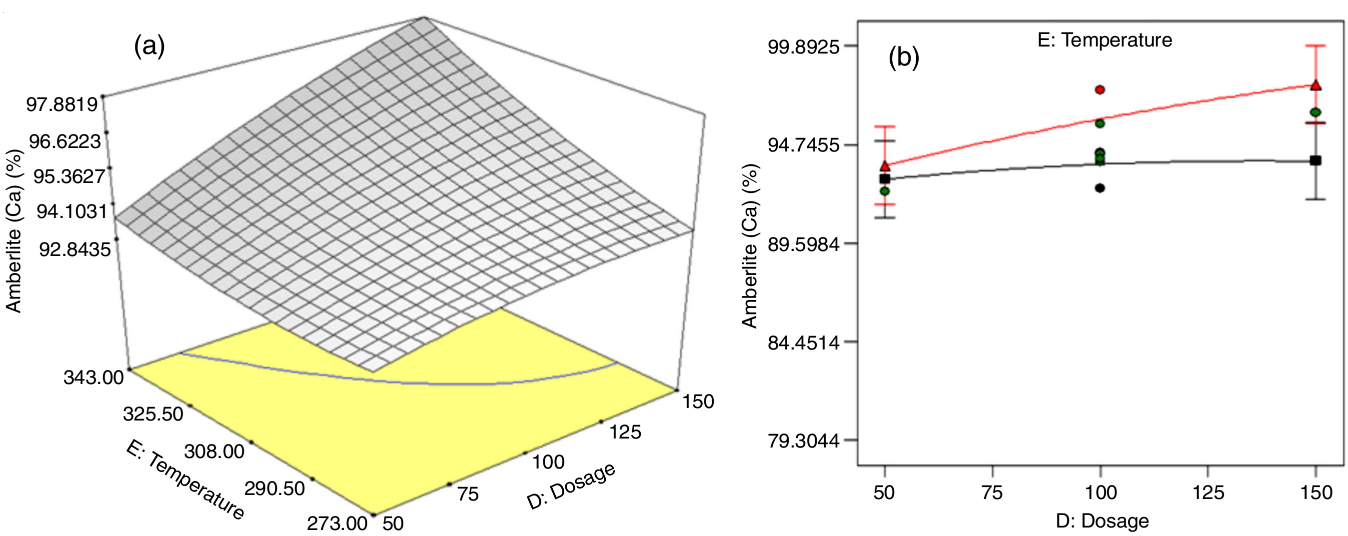

Fig. 7. Effect of temperature and dosage on the removal of Ca^{2+} using Amberlite: (a) surface response method and (b) two-dimensional plot

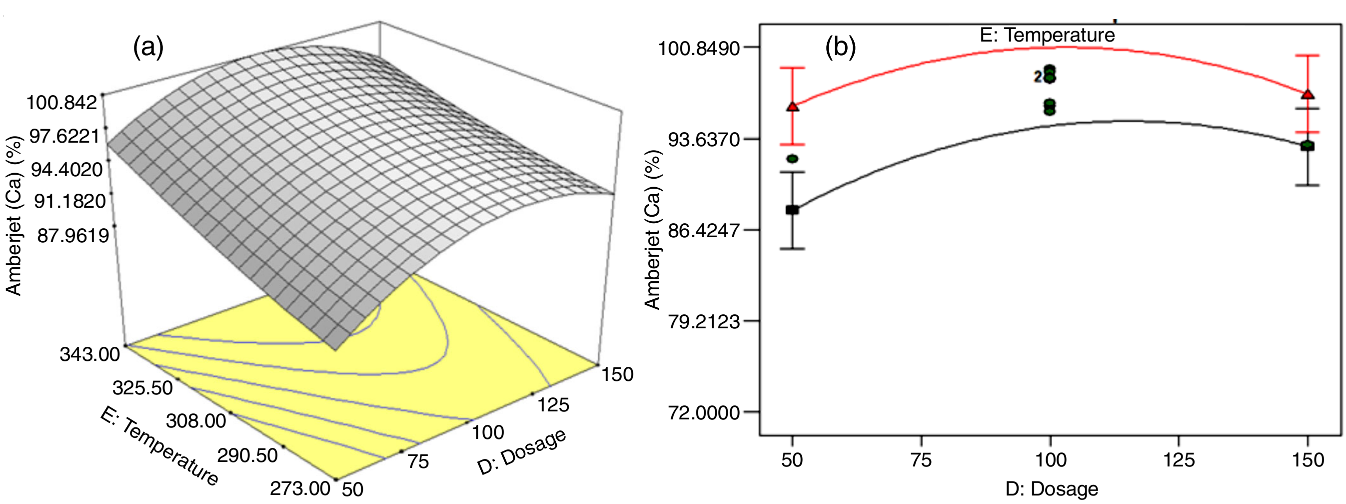

Fig. 8. Effect of temperature and dosage on removing Ca^{2+} using Amberjet: (a) surface response method and (b) two-dimensional plot

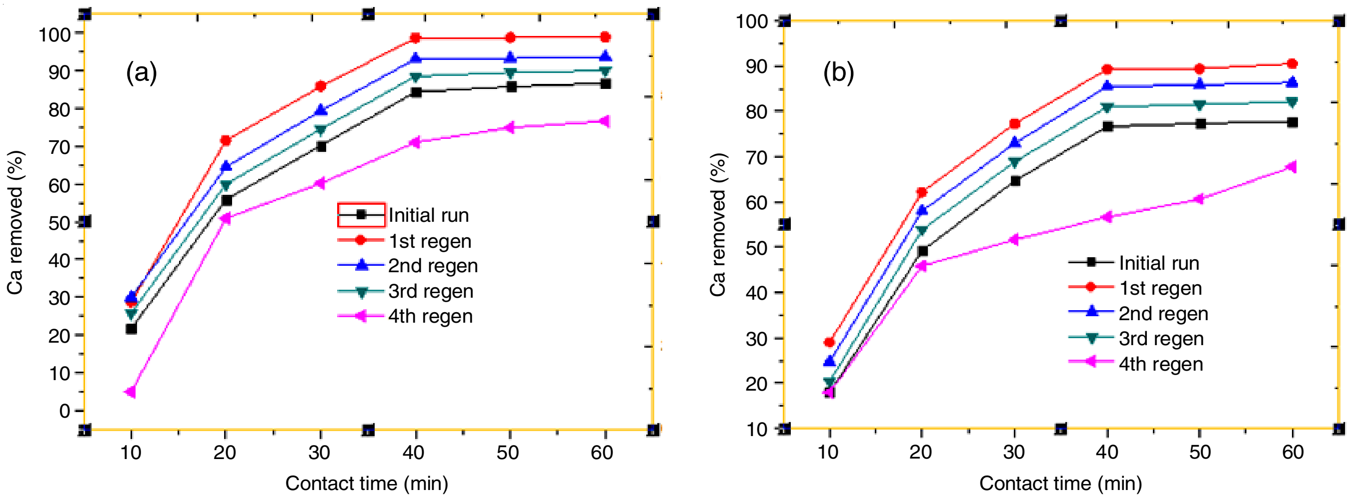

Fig. 9. Regeneration of Amberlite IR1200 (a) and Amberjet 1200 (b) resins on removing Ca^{2+} at conc. = 600 mg/L, dosage = 15 mL, pH = 3 and temp. = 25 °C

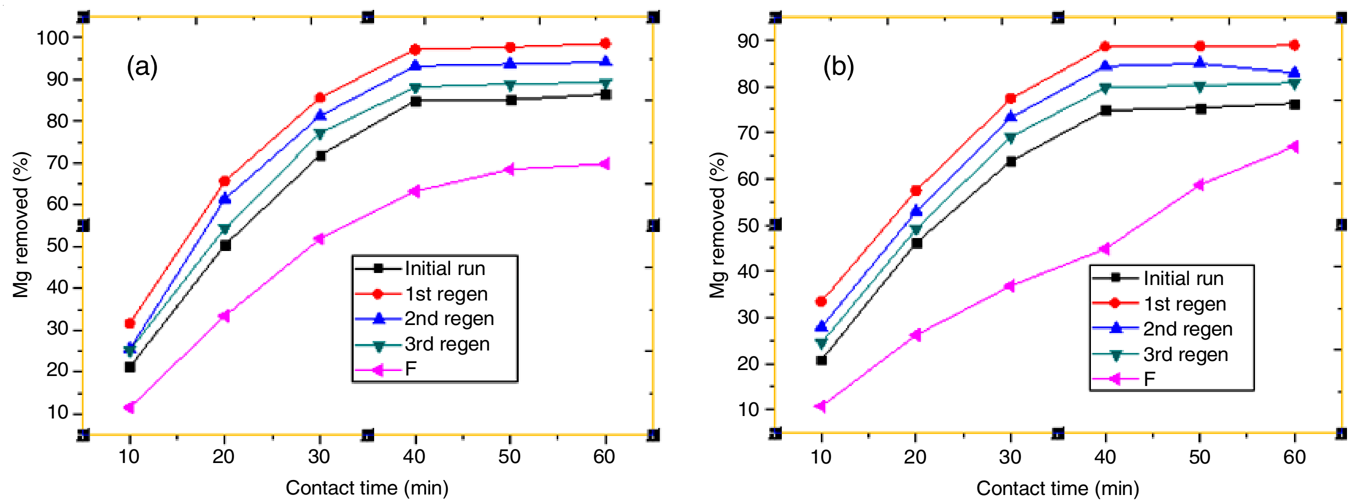

Fig. 10. Regeneration of Amberlite IR1200 (a) and Amberjet 1200 resins (b) on removing Mg^{2+} ions at conc. = 600 mg/L, dosage = 15 mL, pH = 3 and temp. = 25 ºC

second and third regenerations for both Amberlite IR1200 and Amberjet 120 was 89.56, 86.6, 80.56 and 89.65, 86.56, 81.56, respectively. However, the highest % Mg^{2+} removal of the fourth regenerations on Amberlite IR1200 and Amberjet 120 were found to be 56.89 and 59.56, which were lower than the results of the initial runs. This suggests that Na^+-form resins has nearly all saturated exchangeable sites or 0.5NaCl could not regenerate effectively. Consequently, the regeneration of the Na^+ component of Amberlite IR1200 and Amberjet 120 may have provided only few sites for further ion exchange. Similar patterns were also observed in the removal of heavy metals through the utilization of clinoptilolite [30].

Conclusion

This study showed that it is possible to remove Ca^{2+} and Mg^{2+} from cooling tower water using Amberlite IR120 and Amberjet 1200 and optimized the process using response surface methodology. Regeneration of the resins was also conducted. The performance of this process is highly dependent on the proper selection and optimization of the process variables. The central composite design, a statistical tool in response surface methodology, proved a valuable for finding the optimal conditions for the ion exchange. The optimal ion exchange operating conditions for Amberlite IR120 and Amberjet 1200 were found to be: contact time was 120 min, dosage of 150 mL, the initial pH level of 2, a concentration of 4.00 mg/L and temperature of 343 K. Regeneration of Amberlite IR120 and Amberjet 1200 using 0.5 M NaCl stripping solution initially showed an increase in % Ca^{2+} and Mg^{2+} removal, then a decrease in subsequent cycles.

CONFLICT OF INTEREST

The authors declare that there is no conflict of interests regarding the publication of this article.

REFERENCES

1. D.E. Kimbrough and I.H. Suffet, *Environ. Sci. Technol.*, **29**, 2217 (1995); https://doi.org/10.1021/es00009a010
2. S.F. Ahmed, P.S. Kumar, M.R. Rozbu, A.T. Chowdhury, S. Nuzhat and N. Rafa, *Environ. Technol. Innov.*, **25**, 102114 (2022); https://doi.org/10.1016/j.eti.2021.102114

3. R. González-Gómez, A. Ortega, L.M. Lazo and G. Burillo, *Radiat. Phys. Chem.*, **102**, 117 (2014); https://doi.org/10.1016/j.radphyschem.2014.04.026
4. S.B. Jadhav, A.S. Chougule, D.P. Shah, C.S. Pereira and J.P. Jadhav, *Clean Technol. Environ. Policy*, **17**, 709 (2015); https://doi.org/10.1007/s10098-014-0827-3
5. J. Liu, G. Hu, K. Du, Z. Peng and Y. Cao, *J. Clean. Prod.*, **84**, 746 (2014); https://doi.org/10.1016/j.jclepro.2014.01.062
6. N.A.A. Qasem, R.H. Mohammed and D.U. Lawal, *npj Clean Water*, **4**, 36 (2021); https://doi.org/10.1038/s41545-021-00127-0
7. S. Rengaraj, J.W. Yeon, Y. Kim, Y. Jung, Y.K. Ha and W.H. Kim, *J. Hazard. Mater.*, **143**, 469 (2007); https://doi.org/10.1016/j.jhazmat.2006.09.064
8. S.A. Abo-Farha, A.Y. Abdel-Aal, I.A. Ashour and S.E. Garamon, *J. Hazard. Mater.*, **169**, 190 (2009); https://doi.org/10.1016/j.jhazmat.2009.03.086
9. K.C. Khulbe and T. Matsuura, *Appl. Water Sci.*, **8**, 19 (2018); https://doi.org/10.1007/s13201-018-0661-6
10. L. Malise, H. Rutto, T. Seodigeng, L. Sibali abd P. Ndibewu, *Chem. Eng. Trans.*, **82**, 421 (2020); https://doi.org/10.3303/CET2082071
11. M. Banza and H. Rutto, *J. Environ. Sci. Health Part A Tox. Hazard. Subst. Environ. Eng.*, **57**, 117 (2022); https://doi.org/10.1080/10934529.2022.2036552
12. H. Rutto, T. Seidigeng and L. Malise, *Arch. Environ. Prot.*, **45**, 92 (2023); https://doi.org/10.24425/aep.2019.130245
13. S.R. Devi and M.N.V. Prasad, *Heavy Met. Stress Plants*, **144**, 99 (1999); https://doi.org/10.1007/978-3-662-07745-0_5
14. S. Kumar and S. Jain, *J. Chem.*, 2013, 957647 (2013); https://doi.org/10.1155/2013/957647
15. R. Marr and T. Gamse, *Chem. Eng. Process.*, **39**, 19 (2000); https://doi.org/10.1016/S0255-2701(99)00070-7
16. E. Pehlivan and T. Altun, *J. Hazard. Mater.*, **134**, 149 (2006); https://doi.org/10.1016/j.jhazmat.2005.10.052
17. E. Maliou, M. Malamis and P.O. Sakellarides, *Water Sci. Technol.*, **25**, 133 (1992); https://doi.org/10.2166/wst.1992.0020
18. J.P. Chen and L. Wang, *Sep. Sci. Technol.*, **36**, 3617 (2001); https://doi.org/10.1081/SS-100108352
19. P. Outola, H. Leinonen, M. Ridell and J. Lehto, *Solvent Extr. Ion Exch.*, **19**, 743 (2001); https://doi.org/10.1081/SEI-100103818
20. P. Woodberry, G. Stevens, I. Snape and I. Stark, *Solvent Extr. Ion Exch.*, **23**, 289 (2005); https://doi.org/10.1081/SEI-200044387
21. A. Agrawal, K.K. Sahu and J.P. Rawat, *Solvent Extr. Ion Exch.*, **21**, 763 (2003); https://doi.org/10.1081/SEI-120024556
22. M. Laikhtman, J. Riviello and J.S. Rohrer, *J. Chromatogr. A*, **816**, 282 (1998); https://doi.org/10.1016/S0021-9673(98)00530-5
23. C. Özmetin, Ö. Aydin, M.M. Kocakerim, M. Korkmaz and E. Özmetin, *Chem. Eng. J.*, **148**, 420 (2009); https://doi.org/10.1016/j.cej.2008.09.021
24. A.P. Kryvoruchko, I.D. Atamanenko and L.Y. Yurlova, *J. Membr. Sci.*, **228**, 77 (2004); https://doi.org/10.1016/j.memsci.2003.09.013
25. W. Jiang, J.A. Joens, D.D. Dionysiou and K.E. O'Shea, *J. Photochem.*, **262**, 7 (2013); https://doi.org/10.1016/j.jphotochem.2013.04.008
26. M.A. Islam, V. Sakkas and T.A. Albanis, *J. Hazard. Mater.*, **170**, 230 (2009); https://doi.org/10.1016/j.jhazmat.2009.04.106
27. V. Petrovic, V. Opacic-Galic, S. Zivkovic, B. Nikolic, V. Danilovic, V. Miletic, V. Jokanovic and D. Mitic-Culafic, *Int. Endodontic J.*, **48**, 966 (2015); https://doi.org/10.1111/iej.12391
28. M. Borandegi and A. Nezamzadeh-Ejhieh, *Colloids Surf. A Physicochem. Eng. Asp.*, **479**, 35 (2015); https://doi.org/10.1016/j.colsurfa.2015.03.040
29. M. Argun, *J. Hazard. Mater.*, **150**, 587 (2008); https://doi.org/10.1016/j.jhazmat.2007.05.008
30. C.H. Giles, A.P. D'Silva and I.A. Easton, *J. Colloid Interface Sci.*, **47**, 766 (1974); https://doi.org/10.1016/0021-9797(74)90253-7